

Stability Analysis of Thin Electrically-Conductive Viscoelastic Fluid Film Flow Along a Rotating Cylinder in a Magnetic Field

Wu-Man Liu* and Cha'o-Kuang Chen**

Keywords : Hydromagnetic stability analysis, Hartmann number, Rossby number

ABSTRACT

In this study, stability of thin electrically-conductive viscoelastic fluid film flow along the side of a rotating vertical cylinder with the effect of magnetic field is discussed in this paper. This paper applied long-wave perturbation method to solve generalized nonlinear motion equation of thin film. The criteria for linear thin film stability can be obtained by normal mode method, then the multiple-scales method is applied to confirm the nonlinear stability. By the coefficient in Ginzburg-Landau equation, different states of the thin film can be determined. From this study, in order to enhance the stability of the thin film, it can be achieved by either increasing the effect of the magnetic field, decreasing the viscoelastic effect or decreasing the rotational velocity. Meanwhile, increasing radius under large Rossby number can lead to losing stability easier, such as the dimensionless radius is more than 50. It is worth noting that this phenomenon is led by the radius, and the influence is stronger than other parameters.

INTRODUCTION

The topic of flow stability had been studied over the years and specific shapes, different types of fluid, and more complex conditions had been considered in order to obtain results that is closer to reality and have better understanding of thin film fluid.

In recent year, many studies focused on thin film fluid with the effect of magnetic field (Ahmad et al., 2021; Dawar et al., 2022; Khan et al., 2017). The earliest stability of the thin film effected by magnetic field have been discussed in 1996. Study

*Paper Received May., 2022. Revised July, 2022. Accepted July, 2022.
Author for Correspondence: Wu-Man Liu.*

* Ph.D. candidate, Department of Mechanical Engineering, National Cheng Kung University, Tainan, Taiwan, ROC.

** Professor, Department of Mechanical Engineering, National Cheng Kung University, Tainan, Taiwan, ROC.

regards thin film stability can be divided into linear stability and nonlinear stability. Traditional linear theory lost its accuracy when the disturbance becomes larger. Due to the effect of the higher order terms can no longer be neglected, nonlinear theory need to be applied in the analysis. There are many researches that used Ginzburg-Landau Equation in analyzing thin film stability (Chen et al., 2004; Chen and Lin, 2009; Cheng, 2009). Models for non-Newtonian fluid proposed by different researchers may varies due to their point of view. Such as Ostwald-de Waele power law model (1893), Maxwell fluid model (1867), Bingham Herschel-Bilkly(1922), Carreau fluid model (1972), Eyring-Powell model (1994). Viscoelastic fluid is a kind of which is not only has the viscous property of fluid on its normal and tangential direction, but it also has the elastic property similar to solid. These properties have been widely used in designing bearing, gear and cam. Stability of the viscoelastic thin film fluid had been studied in 2000 (Chen et al., 2000), and some results with other conditions had been obtained (Cheng and Lin, 2007; Lin, 2012). In this paper, stability of thin electrically-conductive viscoelastic fluid film flow along the side of a rotating vertical cylinder with the effect of magnetic field is discussed.

GENERALIZED KINEMATIC EQUATIONS

Due to the existence of electromagnetic inductance, electrically conductive magnetofluid films cause an inductive response when they pass through a magnetic field, and cause a change in the surrounding magnetic field at the same time. The resulting electromagnetic coupling effect is a relatively complex problem. It is a combination of fluid mechanics and electromagnetism. In magneto-fluid mechanics, Maxwell's equations can be written in the following forms.

$$\nabla \cdot \vec{B}^* = 0 \quad (1)$$

$$\nabla \times \vec{H}^* = \vec{j}^* \quad (2)$$

$$\nabla \times \vec{E}^* = -\frac{\partial \vec{B}^*}{\partial t^*} \quad (3)$$

Where \vec{J}^* is the current density and \vec{H}^* is the intensity of the magnetic field. Furthermore, \vec{B}^* is the magnetic flux, and given by

$$\vec{B}^* = \mu_e^* \vec{H}^* \quad (4)$$

where μ_e^* is the magnetic permeability and \vec{E}^* is the intensity of the electric field. From Ohm's law, the total current flow is given by

$$\vec{J}^* = \sigma^* (\vec{E}^* + \vec{V}^* \times \vec{B}^*) \quad (5)$$

where \vec{V}^* is the velocity vector and $\vec{\sigma}^*$ is the electrical conductivity. By combining Eqs. (1) ~ (5) and replacing \vec{H}^* by \vec{B}^*/μ_e^* , the following magnetic induction equation can be obtained:

$$\frac{\partial \vec{B}^*}{\partial t^*} = \nabla \times (\vec{V}^* \times \vec{B}^*) + \frac{1}{\sigma^* \mu_e^*} \nabla^2 \vec{B}^* \quad (6)$$

If no polarization voltage is applied (i.e., $\vec{E}^* = 0$), the electromagnetic force F_m^* acting on the falling fluid film is given by

$$F_m^* = \vec{J}^* \times \vec{B}^* = \sigma^* (\vec{V}^* \times \vec{B}^*) \times \vec{B}^* \quad (7)$$

Furthermore, the Navier-Stokes equation for the fluid film can be expressed as

$$\rho^* \left(\frac{\partial \vec{V}^*}{\partial t^*} + \vec{V}^* \cdot \nabla \vec{V}^* \right) = \rho^* \vec{g}^* + \nabla \vec{\tau}^* + \sigma^* (\vec{V}^* \times \vec{B}^*) \times \vec{B}^* \quad (8)$$

where $\vec{\tau}^*$ is the Cauchy stress tensor.

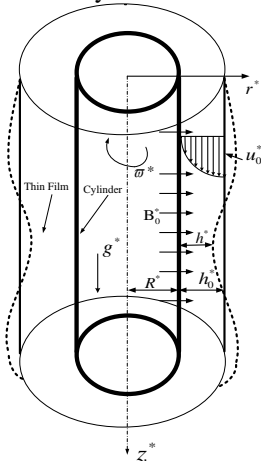


Fig. 1 Schematic of thin electrically-conductive viscoelastic film flowing down outer surface of rotating vertical cylinder in magnetic field

Figure 1 is a schematic diagram. There is a rotating infinitely long cylinder in the middle with a thin film of electrically-conductive viscoelastic fluid flowing down its surface and a magnetic field perpendicular to the cylinder surface. The whole system is axisymmetric. Assuming the magnetic Reynolds number ($Re_m = \sigma^* \mu_e^* u_0^* h_0^*$) is small, so that the induced magnetic field is negligible compared to the applied magnetic field. Also, it is assumed that the fluid properties do not change with time and that the applied magnetic field is uniform. The continuity equation and momentum equation of the system can be written in the following form.

$$\frac{1}{r^*} \frac{\partial(r^* u^*)}{\partial r^*} + \frac{\partial w^*}{\partial z^*} = 0 \quad (9)$$

$$\rho^* \left(\frac{\partial u^*}{\partial t^*} + u^* \frac{\partial u^*}{\partial r^*} + w^* \frac{\partial u^*}{\partial z^*} - \frac{v^{*2}}{r^*} \right) = \frac{1}{r^*} \frac{\partial(r^* \tau_{r^* r^*}^*)}{\partial r^*} + \frac{\partial \tau_{z^* z^*}^*}{\partial z^*} - \frac{1}{r^*} \tau_{\theta^* \theta^*}^* \quad (10)$$

$$\rho^* \left(\frac{\partial w^*}{\partial t^*} + u^* \frac{\partial w^*}{\partial r^*} + w^* \frac{\partial w^*}{\partial z^*} \right) = \frac{1}{r^*} \frac{\partial(r^* \tau_{r^* z^*}^*)}{\partial r^*} + \frac{\partial \tau_{z^* z^*}^*}{\partial z^*} + \rho^* g^* - \sigma^* B_0^{*2} w^* \quad (11)$$

Where u^* is the velocity of the r^* direction, w^* is the velocity of the z^* direction, ρ^* is a constant density of the fluid, t^* is the time, and g^* is the gravitational acceleration, σ^* is the electrical conductivity, and B_0^* is the magnetic flux density.

According to $F_z^* = -\sigma^* B_0^{*2} w^*$, it can be concluded that the downward flowing fluid is subjected to electromagnetic forces in the opposite direction. Thus, it can be assumed that the tangential velocity is constant in the radial direction of the thin film flow, i.e., $v^* = R^* \Omega^*$, where Ω^* is the angular velocity of the rotating cylinder.

The individual stress components can be written as

$$\tau_{r^* r^*}^* = -p^* + 2\mu_0^* \frac{\partial u^*}{\partial r^*} - 2k_0^* \left[\frac{\partial^2 u^*}{\partial t^* \partial r^*} + u^* \frac{\partial^2 u^*}{\partial r^{*2}} + w^* \frac{\partial^2 u^*}{\partial r^* \partial z^*} - 2 \left(\frac{\partial u^*}{\partial r^*} \right)^2 - \frac{\partial u^*}{\partial z^*} \left(\frac{\partial u^*}{\partial z^*} + \frac{\partial w^*}{\partial r^*} \right) \right] \quad (12)$$

$$\tau_{z^* z^*}^* = -p^* + 2\mu_0^* \frac{\partial w^*}{\partial z^*} - 2k_0^* \left[\frac{\partial^2 w^*}{\partial t^* \partial z^*} + u^* \frac{\partial^2 w^*}{\partial r^* \partial z^*} + w^* \frac{\partial^2 w^*}{\partial z^{*2}} - 2 \left(\frac{\partial w^*}{\partial z^*} \right)^2 - \frac{\partial w^*}{\partial r^*} \left(\frac{\partial w^*}{\partial r^*} + \frac{\partial u^*}{\partial z^*} \right) \right] \quad (13)$$

$$\tau_{r^* z^*}^* = \tau_{z^* r^*}^* = \mu_0^* \left(\frac{\partial u^*}{\partial z^*} + \frac{\partial w^*}{\partial r^*} \right) - k_0^* \left[\frac{\partial^2 u^*}{\partial t^* \partial z^*} + u^* \left(\frac{\partial^2 w^*}{\partial r^{*2}} + \frac{\partial^2 w^*}{\partial r^* \partial z^*} \right) + w^* \left(\frac{\partial^2 w^*}{\partial r^* \partial z^*} + \frac{\partial^2 u^*}{\partial z^{*2}} \right) - 2 \frac{\partial u^*}{\partial z^*} \frac{\partial w^*}{\partial z^*} - 2 \frac{\partial w^*}{\partial r^*} \frac{\partial u^*}{\partial r^*} - \left(\frac{\partial u^*}{\partial r^*} + \frac{\partial w^*}{\partial z^*} \right) \left(\frac{\partial w^*}{\partial r^*} + \frac{\partial u^*}{\partial z^*} \right) \right] \quad (14)$$

$$\tau_{\theta^* \theta^*}^* = -p^* + 2\mu_0^* \frac{u^*}{r^*} - 2k_0^* \left(\frac{1}{r^*} \frac{\partial u^*}{\partial t^*} + \frac{u^*}{r^*} \frac{\partial u^*}{\partial r^*} - \frac{u^{*2}}{r^{*2}} + \frac{w^*}{r^*} \frac{\partial u^*}{\partial z^*} \right) \quad (15)$$

Where μ_0^* being the limiting dynamic viscosity at small rates of shear and k_0^* is a viscoelastic coefficient, and p^* is the flow pressure.

The no-slip boundary conditions on the outer wall of the cylinder at $r^* = R^*$ are given as

$$u^* = 0 \quad (16)$$

$$w^* = 0 \quad (17)$$

Meanwhile, the boundary conditions at the free surface of the fluid film (i.e., $r^* = R^* + h^*$) are given as (Edwards et al., 1991)

$$\frac{\partial h^*}{\partial z^*} \left[1 + \left(\frac{\partial h^*}{\partial z^*} \right)^2 \right]^{-1} (\tau_{r^* r^*}^* - \tau_{z^* z^*}^*) + \left[1 - \left(\frac{\partial h^*}{\partial z^*} \right)^2 \right] \left[1 + \left(\frac{\partial h^*}{\partial z^*} \right)^2 \right]^{-1} \tau_{r^* z^*}^* = 0 \quad (18)$$

Solving the balance equation in the direction normal to the free surface, it can be shown that the resulting normal stress condition is given by

$$\left[1 + \left(\frac{\partial h^*}{\partial z^*} \right)^2 \right]^{-1} \left[2\tau_{r^* z^*}^* \frac{\partial h^*}{\partial z^*} - \tau_{r^* r^*}^* - \tau_{z^* z^*}^* \left(\frac{\partial h^*}{\partial z^*} \right)^2 \right] + S^* \left\{ \frac{\partial^2 h^*}{\partial z^{*2}} \left[1 + \left(\frac{\partial h^*}{\partial z^*} \right)^2 \right]^{-3/2} - \frac{1}{r^*} \left[1 + \left(\frac{\partial h^*}{\partial z^*} \right)^2 \right]^{-1/2} \right\} = p_a \quad (19)$$

Since the flow cannot travel across the free surface, it follows that

$$\frac{\partial h^*}{\partial t^*} + \frac{\partial h^*}{\partial z^*} w^* - u^* = 0 \quad (20)$$

Where h^* is the local film thickness, P_a^* is the atmospheric pressure, and S^* is the surface tension of the film fluid. Note that the superscripts “*” indicate that the corresponding variables are dimensional quantities. Introducing the stream function ϕ^* , the dimension velocity components become

$$u^* = \frac{1}{r^*} \frac{\partial \phi^*}{\partial z^*}, \quad w^* = -\frac{1}{r^*} \frac{\partial \phi^*}{\partial r^*} \quad (21)$$

For convenience, the following dimensionless quantities are defined:

$$\begin{aligned} r &= \frac{r^*}{h_0^*}, \quad z = \frac{\alpha z^*}{h_0^*}, \quad t = \frac{\alpha u_0^* t^*}{h_0^*}, \quad h = \frac{h^*}{h_0^*}, \quad \phi = \frac{\phi^*}{u_0^* h_0^{*2}}, \\ p &= \frac{p^* - p_a^*}{\rho u_0^{*2}}, \quad Re = \frac{u_0^* h_0^*}{\nu_0^*}, \quad S = \left(\frac{S^*}{2^2 \rho^{*3} \nu_0^{*4} g^*} \right)^{1/3}, \\ \alpha &= \frac{2\pi h_0^*}{\lambda^*}, \quad R = \frac{R^*}{h_0^*}, \end{aligned} \quad (22)$$

where Re is the Reynolds number, R is the dimensionless radius of the cylinder, λ^* is the perturbed wavelength, ν_0^* is the kinematic viscosity of the fluid, α is the dimensionless wave number, S is dimensionless surface tension, h_0^* is the film thickness of the local base flow, and u_0^* is the reference velocity, and is defined as

$$u_0^* = \frac{g^* h_0^{*2}}{4\nu_0^* \Gamma} \quad (23)$$

where

$$\Gamma = [2(1+R)^2 \ln\left(\frac{1+R}{R}\right) - (1+2R)]^{-1} \quad (24)$$

To find the effects of angular velocity, Ω^* , the applied magnetic field, B_0^* , and the viscoelastic coefficient k_0^* on the stability of the flow system, the dimensionless Rossby number, β , the Hartmann number, m , and the viscoelastic parameter, k are introduced

$$\beta = \frac{\Omega^* h_0^*}{u_0^*}, \quad m = \left(\frac{\sigma^* B_0^{*2} h_0^{*2}}{\rho^* \nu_0^*} \right)^{1/2}, \quad k = \frac{k_0^*}{\rho^* h_0^{*2}}. \quad (25)$$

Thus, the non-dimensional governing equations for the fluid film system are obtained as

$$p_r = \alpha [Re^{-1}(r^{-1}\phi_{rrz} - r^{-2}\phi_{rz})] + \frac{(R\beta)^2}{r} + O(\alpha^2) \quad (26)$$

$$\begin{aligned} r^{-1}(r(r^{-1}\phi_r)_r)_r - \frac{m}{r}\phi_r &= 4\Gamma + \alpha Re[-p_z + \\ r^{-1}\phi_{tr} + r^{-2}\phi_z\phi_{rr} - r^{-3}\phi_z\phi_r - r^{-2}\phi_r\phi_{rz} + \\ k(3r^{-5}\phi_r\phi_z - 3r^{-4}\phi_z\phi_{rr} - 3r^{-4}\phi_r\phi_{rz} + \\ 2r^{-3}\phi_{rz}\phi_{rr} - r^{-2}\phi_{rz}\phi_{rrr} + r^{-2}\phi_z\phi_{rrrr} + \\ r^{-2}\phi_{rr}\phi_{rrz} - r^{-2}\phi_r\phi_{rrrz} + r^{-3}\phi_{tr} - r^{-2}\phi_{trr} + \\ r^{-1}\phi_{trrr})] + O(\alpha^2) \end{aligned} \quad (27)$$

The corresponding boundary conditions are given as follows:

$$\begin{aligned} \text{At the cylinder surface } (r = R) \\ \phi = \phi_r = \phi_z = 0 \end{aligned} \quad (28)$$

$$\begin{aligned} \text{At the free surface } (r = R + h) \\ (r^{-1}\phi_r)_r = \alpha \cdot Re \cdot k [(-2r^{-4}\phi_r^2 + 4r^{-3}\phi_r\phi_{rr} - \\ 2r^{-2}\phi_{rr}^2)h_z - r^{-4}\phi_z\phi_r + r^{-3}\phi_z\phi_{rr} + r^{-2}\phi_z\phi_{rrr} + \\ 3r^{-3}\phi_r\phi_{rz} - r^{-2}\phi_r\phi_{rrz} - 2r^{-2}\phi_{rr}\phi_{rz} - r^{-2}\phi_{tr} + \\ r^{-1}\phi_{trr}] + O(\alpha^2) \end{aligned} \quad (29)$$

$$\begin{aligned} p = -2S \cdot Re^{-5/3} (2\Gamma)^{1/3} (\alpha^2 h_{zz} - r^{-1}) + \\ \alpha \{ [-2Re^{-1} [(r^{-2}\phi_r - r^{-1}\phi_{rr})h_z + r^{-2}\phi_z - \\ r^{-1}\phi_{rz}]] + O(\alpha^2) \end{aligned} \quad (30)$$

$$h_t - r^{-1}(\phi_r h_z + \phi_z) = 0 \quad (31)$$

For nonlinear analysis of thin-film flows, the long-

wavelength modes that provide the minimum wave number, α , are the most probable to cause instability in the flow. Expanding the above equation with the dimensionless stream function, ϕ , and pressure, p , by small wave number α will be shown below:

$$\phi = \phi_0 + \alpha\phi_1 + O(\alpha^2) \quad (32)$$

$$p = p_0 + \alpha p_1 + O(\alpha^2) \quad (33)$$

Substituting Eq. (32) and (33) into Eq. (26) ~ (31), the governing equations of the thin-film system can be collected and solved on an order-by-order basis. In practice, the non-dimensional surface tension, S , has a large value, and thus the term $\alpha^2 S$ can be treated as a zeroth-order quantity (Chen *et al.*, 2004; 2005; Tsai *et al.*, 1996). Furthermore, for $r - R \leq h$, the film thickness is very small, and hence power-series approximation solutions can be obtained up to the order of $(r - R)^5$ at the zeroth- and first-order of the stream function. Then, the Zeroth-order solution can be obtained:

$$\begin{aligned} \phi_0 = (r - R)^2 \Gamma \{ 2hR^2(h - 2R) - 2/3(r - R)R\Phi + \\ 1/6(r - R)^2[4R^2 + 3h^2(1 + mR^2) - 2h(R + \\ mR^3)] - 4/15(r - R)^3(q + mhR^2) \} / \Omega \end{aligned} \quad (34)$$

where

$$\begin{aligned} \Phi = 2R^2 - 4hR + (3 + mR^2)h^2, \quad q = R + h, \quad \Omega = \\ 2R^2 - 2hR + (2 + mR^2)h^2 \end{aligned} \quad (35)$$

First-order solution:

$$\begin{aligned} \phi_1 = C_2(r - R)^2 + C_3(r - R)^3 + C_4(r - R)^4 + \\ C_5(r - R)^5 \end{aligned} \quad (36)$$

where the $C_2 \sim C_5$ are given in the Appendix A.

Substituting the solutions of the zeroth- and first-order equations into the dimensionless free surface kinematic equation given in Eq. (31), the following generalized nonlinear kinematic equation can be obtained:

$$\begin{aligned} h_t + A(h)h_z + B(h)h_{zz} + C(h)h_{zzzz} + D(h)h_z^2 + \\ E(h)h_z h_{zz} = 0 \end{aligned} \quad (37)$$

where $A(h), B(h), C(h), D(h)$ and $E(h)$ are given in Appendix B.

The Rossby number represents the rotation of the cylinder, when the Rossby number is zero, it means that the fluid film is flowing down the stationary cylinder. The Hartmann number represents the strength of the magnetic field, and when the Hartmann number is 0, it means that the fluid film is flowing downward in the absence of the magnetic field. k is related to the viscoelasticity of the fluid, and when k is 0, it means that only viscous effects are left in the fluid film.

After zeroing these parameters, the results can be compared with those of other authors under the corresponding conditions.

STABILITY ANALYSIS

In this paper, the dimensionless film thickness in the small perturbed state will be expressed as the following equation:

$$h(t, z) = 1 + \eta(t, z), \quad \eta = O(\alpha) \quad (38)$$

where η is the perturbation quantity of the stationary film thickness. By substituting Eq. (38) into Eq. (37) and collecting all the terms up to the order of 3, the η can be obtained as

$$\eta_t + A\eta_z + B\eta_{zz} + C\eta_{zzzz} + D\eta_z^2 + E\eta_z\eta_{zzz} = -[(A'\eta + \frac{A''}{2}\eta^2)\eta_z + (B'\eta + \frac{B''}{2}\eta^2)\eta_{zz} + (C'\eta + \frac{C''}{2}\eta^2)\eta_{zzzz} + (D + D'\eta)\eta_z^2 + (E + E'\eta)\eta_z\eta_{zzz}] + O(\eta^4) \quad (39)$$

Note that the values of A, B, C, D and E and their corresponding derivatives are all evaluated at the dimensionless height $h=1$ of the film flow.

Linear Stability Analysis

Neglecting the nonlinear terms in Eq. (39), the following linearized equation can be obtained

$$\eta_t + A\eta_z + B\eta_{zz} + C\eta_{zzzz} = 0 \quad (40)$$

In order to analyze the linear stability characteristics of the thin film using the normal mode method, an assumption is made that

$$\eta = a \exp[i(z - dt)] + c.c. \quad (41)$$

where a is the perturbation amplitude and $c.c.$ denotes its complex conjugate counterpart. The complex wave celerity, d , is given as

$$d = d_r + id_i = A + i(B - C) \quad (42)$$

where d_r is the linear wave speed and d_i is the linear growth rate of the wave amplitude. For $d_i > 0$, the flow is in an unstable linearly supercritical condition. Conversely, for $d_i < 0$, the flow is in a stable linearly subcritical condition.

Nonlinear Stability Analysis

The nonlinear stability of the thin-film system is analyzed by the multiple-scales method. The associated notations are defined as

$$\frac{\partial}{\partial t} \rightarrow \frac{\partial}{\partial t} + \varepsilon \frac{\partial}{\partial t_1} + \varepsilon^2 \frac{\partial}{\partial t_2} \quad (43)$$

$$\frac{\partial}{\partial z} \rightarrow \frac{\partial}{\partial z} + \varepsilon \frac{\partial}{\partial z_1} \quad (44)$$

$$\eta(\varepsilon, z, z_1, t, t_1, t_2) = \varepsilon\eta_1 + \varepsilon^2\eta_2 + \varepsilon^3\eta_3 \quad (45)$$

where ε is a small perturbation parameter, $t_1 = \varepsilon t$, $t_2 = \varepsilon^2 t$ and $z_1 = \varepsilon z$. Substituting the expressions above Eq. (43) ~ (45) into Eq. (39) and then expanding and rearranging yields the following equation:

$$(L_0 + \varepsilon L_1 + \varepsilon^2 L_2)(\varepsilon\eta_1 + \varepsilon^2\eta_2 + \varepsilon^3\eta_3) = -\varepsilon^2 N_2 - \varepsilon^3 N_3 \quad (46)$$

where

$$L_0 = \frac{\partial}{\partial t} + A \frac{\partial}{\partial z} + B \frac{\partial^2}{\partial z^2} + C \frac{\partial^4}{\partial z^4} \quad (47)$$

$$L_1 = \frac{\partial}{\partial t_1} + A \frac{\partial}{\partial z_1} + 2B \frac{\partial}{\partial z} \frac{\partial}{\partial z_1} + 4C \frac{\partial^3}{\partial z^3} \frac{\partial}{\partial z_1} \quad (48)$$

$$L_2 = \frac{\partial}{\partial t_2} + B \frac{\partial^2}{\partial z_1^2} + 6C \frac{\partial^2}{\partial z^2} \frac{\partial^2}{\partial z_1^2} \quad (49)$$

$$N_2 = A'\eta_1\eta_{1z} + B'\eta_1\eta_{1zz} + C'\eta_1\eta_{1zzzz} + D\eta_{1z}^2 + E\eta_{1z}\eta_{1zzz} \quad (50)$$

$$N_3 = A(\eta_1\eta_{2z} + \eta_{1z}\eta_2 + \eta_1\eta_{2z_1}) + B'(\eta_1\eta_{2zz} + 2\eta_1\eta_{2zz_1} + \eta_{1zz}\eta_2) + C'(\eta_1\eta_{2zzzz} + 4\eta_1\eta_{2zzz_1} + \eta_{1zzzz}\eta_2) + D(2\eta_{1z}\eta_{2z} + 2\eta_{1z}\eta_{2z_1}) + E(\eta_{1z}\eta_{2zzz} +$$

$$3\eta_{1z}\eta_{2zzz_1} + \eta_{1zzz}\eta_{2z} + \eta_{1zzz}\eta_{2z_1}) + \frac{1}{2}A''\eta_1^2\eta_{1z} + \frac{1}{2}B''\eta_1^2\eta_{1zz} + \frac{1}{2}C''\eta_1^2\eta_{1zzzz} + D'\eta_1\eta_{1z}^2 + E'\eta_1\eta_{1z}\eta_{1zzz} \quad (51)$$

Eq. (46) can then be solved on an order-by-order basis. Collecting all terms of order $O(\varepsilon)$ and solving the resulting equation $L_0\eta_1 = 0$ gives

$$\eta_1 = a(z_1, t_1, t_2) \exp[i(z - d_r t)] + c.c. \quad (52)$$

After collecting terms and solving the secular equation of order $O(\varepsilon^2)$, it can be shown that η_2 is given by

$$\eta_2 = ea^2 \exp[2i(z - d_r t)] + c.c. \quad (53)$$

Substituting η_1 and η_2 into the secular equation of order $O(\varepsilon^3)$, it can be shown that

$$\frac{\partial a}{\partial t_2} + D_1 \frac{\partial^2 a}{\partial z_1^2} - \varepsilon^{-2} d_i a + (E_1 + iF_1)a^2 \bar{a} = 0 \quad (54)$$

where

$$e = e_r + ie_i = (B' - C' + D - E)/(16C - 4B) + iA'/(4B - 16C) \quad (55)$$

$$D_1 = B - 6C \quad (56)$$

$$E_1 = (-5B' + 17C' + 4D - 10E)e_r - A'e_i + (-3B''/2 + 3C''/2 + D' - E') \quad (57)$$

$$F_1 = (-5B' + 17C' + 4D - 10E)e_i + A'e_r + A''/2 \quad (58)$$

Note that the overhead bar in Eq. (54) denotes the complex conjugate of the corresponding variable. Eq. (54) is generally referred to as the Ginzburg-Landau equation (Ginzburg and Landau, 1950). In investigating the weak nonlinear behavior of a fluid film flow, a solution with an exponential form is assumed, i.e.

$$a = a_0 \exp[-ib(t_2)t_2] \quad (59)$$

Employing a filtered wave condition which gives no spatial modulation, neglecting the diffusion term, and substituting the assumed solution of Eq. (59) into Eq. (54), it can be shown that

$$\frac{\partial a_0}{\partial t_2} = (\varepsilon^{-2} d_i - E_1 a_0^2) a_0 \quad (60)$$

$$\frac{\partial [b(t_2)t_2]}{\partial t_2} = F_1 a_0^2 \quad (61)$$

The second term on the right-hand side of Eq. (60) is induced by the nonlinearity effect and causes the exponential growth of the linear disturbance to either decelerate or accelerate depending on the respective signs of d_i and E_1 . Clearly, if E_1 is zero, Eq. (60) reduces to a simple linear equation. Meanwhile, Eq. (61) describes the effect of infinitesimal disturbances within the nonlinear system on the perturbed wave speed. In the linearly unstable region ($d_i > 0$), the necessary condition for the existence of a supercritical stable region is given as $E_1 > 0$. The corresponding threshold amplitude, εa_0 , is defined as

$$\varepsilon a_0 = \sqrt{\frac{d_i}{E_1}} \quad (62)$$

while the nonlinear wave speed is given by

$$Nc_r = d_r + \varepsilon^2 b = d_r + d_i \left(\frac{F_1}{E_1}\right) \quad (63)$$

Conversely, in the linearly stable region ($d_i < 0$), if $E_1 < 0$, the film flow exhibits subcritical instability with a threshold amplitude of εa_0 . The necessary condition for the existence of a subcritical stable region

is given as $E_1 > 0$, while that for a neutral stability curve is given by $E_1 = 0$. Based upon the discussions above, various characteristic states of the Landau equation can be identified, as summarized in Table 1.

Table 1. Characteristic states of Landau equation

linearly stable (subcritical region) $d_i < 0$	subcritical instability $E_1 < 0$	$\varepsilon a_0 < \left(\frac{d_i}{E_1}\right)^{\frac{1}{2}}$	$a_0 \rightarrow 0$	conditional stability
		$\varepsilon a_0 > \left(\frac{d_i}{E_1}\right)^{\frac{1}{2}}$	$a_0 \uparrow$	subcritical explosive state
linearly unstable (supercritical region) $d_i > 0$	subcritical (absolute) Stability $E_1 > 0$	$a_0 \rightarrow 0$		
	supercritical explosive state $E_1 < 0$	$a_0 \uparrow$		
	supercritical stability $E_1 > 0$	$\varepsilon a_0 \rightarrow \left(\frac{d_i}{E_1}\right)^{\frac{1}{2}}$ $Nc_r \rightarrow d_r + d_i \frac{F_1}{E_1}$		

NUMERICAL EXAMPLES

Based on the Maxwell Equation, a calculable mathematical model for thin film of electrically-conductive viscoelastic fluid flowing along a rotating cylinder with the effect of magnetic field can be built, which contains a model for linear stability and nonlinear stability. The mathematical model can then be nondimensionalized. Hartmann number, Rossby number, dimensionless viscoelastic parameter and dimensionless cylinder radius are the parameters that can affect the system. Let the following conditions for the convenience of later computation and analysis:

- (1) Reynolds number $Re = 0 \sim 15$,
- (2) Dimensionless perturbation wave number $\alpha = 0 \sim 0.12$,
- (3) Hartmann number $m = 0, 0.1, \text{ and } 0.2$,
- (4) Rossby number $\beta = 0, 0.1, 0.2, \text{ and } 0.5$,
- (5) Dimensionless viscoelastic parameter $k = 0, 0.1, \text{ and } 0.2$,
- (6) Dimensionless cylinder radius $R = 10, 20, 50, \text{ and } 1000$. The dimensionless surface tension is assumed to have a constant value of $S = 6173.5$ (Tsai *et al.*, 1996).

Linear Stability Analysis

Neutral stability curve is important in determining linear stability of the thin film. In Figure 2, the curve of $d_i = 0$ is the neutral stability curve and it can divide the graph into two regions. On the left side of the curve (i.e., $d_i < 0$), small disturbance within the thin film will shrink and then disappear. The flow remains in laminar flow and stable. On the right side of the curve (i.e., $d_i > 0$), small disturbance within the thin film will grow stronger and then change the flow state from laminar to turbulent. The flow becomes turbulent flow and unstable. Figure 2 (a) ~ (d) show the neutral stability curve of thin film flow system under different Hartmann number, Rossby

number, dimensionless viscoelastic parameter and dimensionless cylinder radius, respectively. For the convenience of comparison, the neutral stability curve with no magnetic field, stationary cylinder and $k = 0$ is added to the graph.

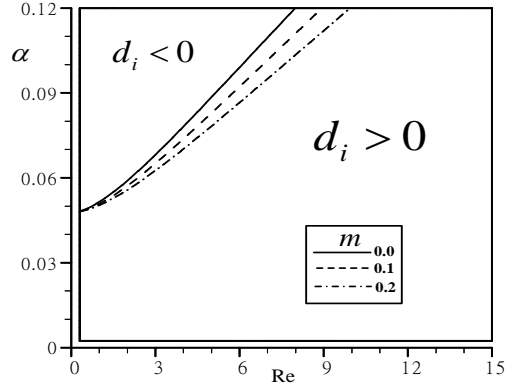


Fig. 2(a) Linear neutral stability curves for three different values of m . ($R=20, k=0.2, \text{ and } \beta=0.2$)

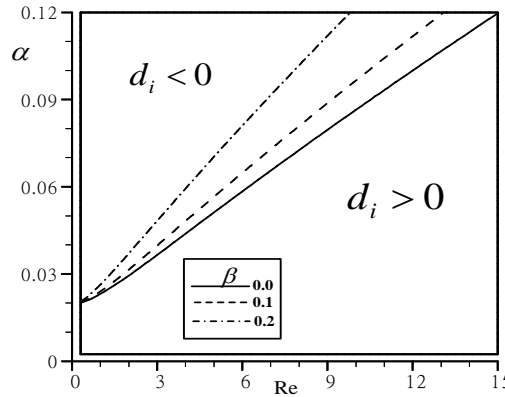


Fig. 2(b) Linear neutral stability curves for three different values of β . ($R=50, m=0.2, \text{ and } k=0.1$)

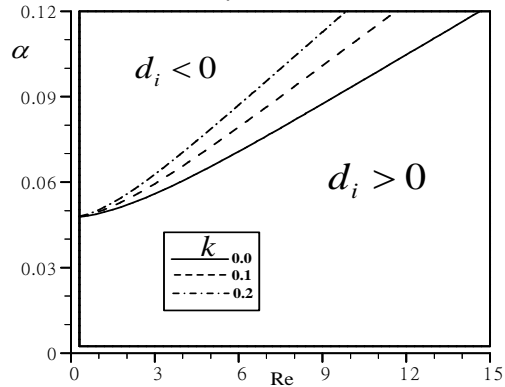


Fig. 2(c) Linear neutral stability curves for three different values of k . ($R=20, m=0.1, \text{ and } \beta=0.1$)

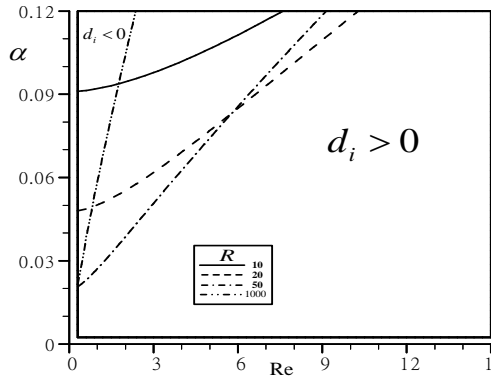


Fig. 2(d) Linear neutral stability curves for four different values of R. ($m=0.1, k=0.1$, and $\beta=0.2$)

Nonlinear Stability Analysis

To analyze Figure 4(a) to 4(d) based on the criteria in Table 1, the thin film system can be divided into 4 regions. In Fig. 4(a) and 4(b), with the increasing of Hartmann number, the linear neutral stability curve shifts downward. Subcritical instability region expands while subcritical stability region and supercritical stability region shift downward, and supercritical explosive state region shrinks. In Fig. 4(a) and 4(c), with the increasing of Rossby number, the linear neutral stability curve grows faster. Subcritical instability region shrinks while subcritical stability region and supercritical stability region shift upward, and supercritical explosive state region expands. In Fig. 4(a) and 4(d), with the decreasing of radius R, the linear neutral stability curve shifts upward significantly. Subcritical instability region shrinks while subcritical stability region and supercritical stability region shift upward, and supercritical explosive state region expands.

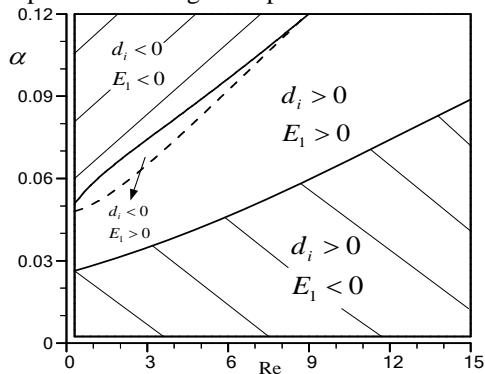


Fig. 4(a) Neutral stability curves for $m=0.1, k=0.2, \beta=0.2$, and $R=20$

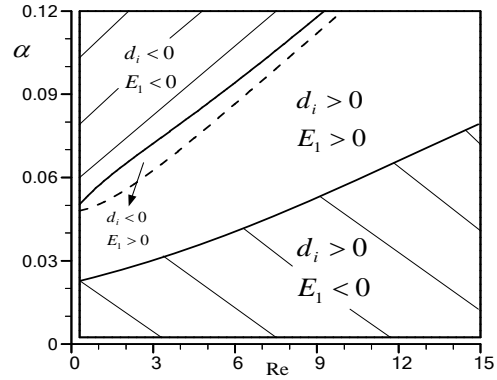


Fig. 4(b) Neutral stability curves for $m=0.2, k=0.2, \beta=0.2$, and $R=20$

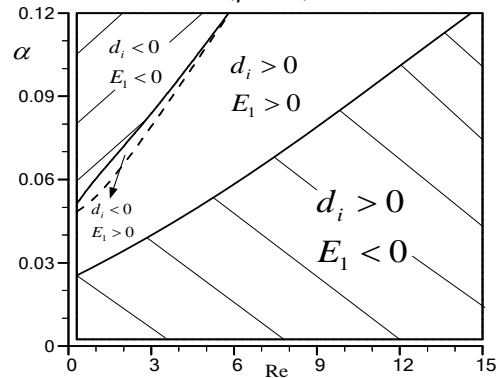


Fig. 4(c) Neutral stability curves for $m=0.1, k=0.2, \beta=0.5$, and $R=20$

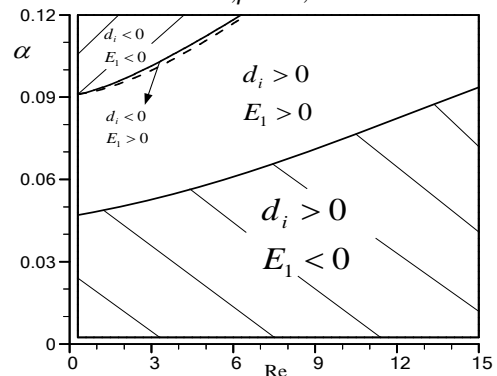


Fig. 4(d) Neutral stability curves for $m=0.1, k=0.2, \beta=0.2$, and $R=10$

Figure 5 shows the variation of threshold amplitude in subcritical unstable region under different wave number. Fig. 5(a) to 5(c) shows threshold amplitude under different Hartmann number, Rossby number and dimensionless radius, respectively. The threshold amplitude increases as Hartmann number increases, but it decreases as Rossby number increases or dimensionless radius increases.

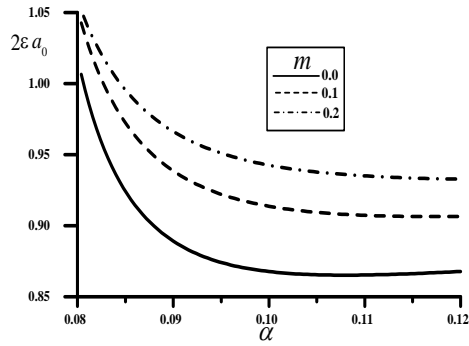


Fig. 5(a) Threshold amplitude in subcritical unstable region for three different values of m . ($Re=3$, $R=20$, $k=0.1$, and $\beta = 0.1$)

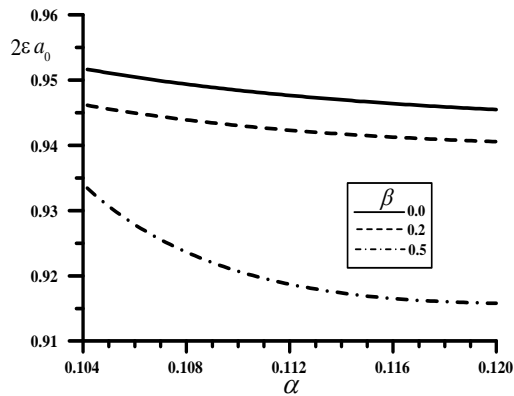


Fig. 5(b) Threshold amplitude in subcritical unstable region for three different values of β . ($Re=3$, $R=50$, $k=0.1$, and $m=0.2$)

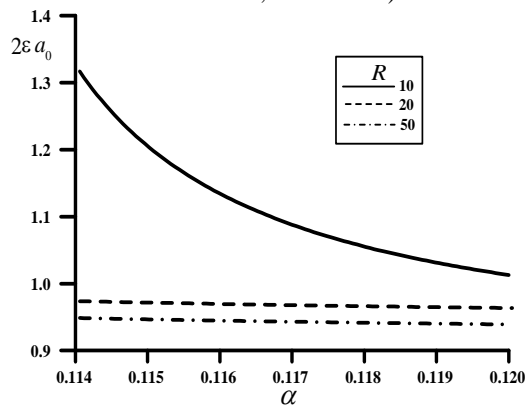


Fig. 5(c) Threshold amplitude in subcritical unstable region for three different values of R . ($Re=6$, $m=0.2$, $\beta = 0.2$, and $k=0.1$)

The stability of the thin film decreases if the threshold amplitude decreases. The system of the thin film remains conditionally stable when initial finite-amplitude disturbance is smaller than threshold amplitude. The system of the thin film becomes explosive unstable when initial finite-amplitude disturbance is greater than threshold amplitude.

Figure 6 analyze the change in threshold amplitude regarding wave number in supercritical stable region.

Fig. 6(a) shows threshold amplitude under different Hartmann number. With Fig. 4(a) and 4(b), wave number and threshold amplitude decrease in supercritical stable region. Fig. 6(b) and 6(c) show threshold amplitude under different Rossby number and viscoelastic parameter. With larger Rossby number and viscoelastic parameter, threshold amplitude increases, and wave number becomes larger in supercritical stable region. Fig. 6(d) and 6(e) show threshold amplitude changes according to radius. In low Rossby number condition, threshold amplitude decreases as radius R becomes larger. In high Rossby number condition, wave number becomes larger and threshold amplitude do not decrease like the others. Higher threshold amplitude results in lower thin film stability.

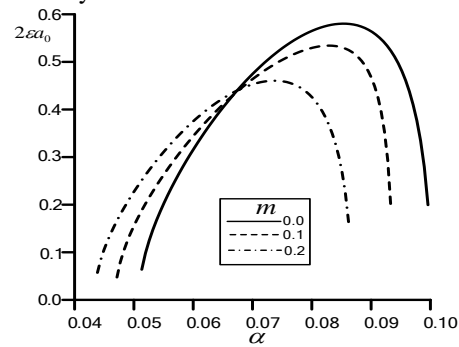


Fig. 6(a) Threshold amplitude in supercritical stable region for three different values of m . ($Re=8$, $\beta=0.1$, $k=0.1$, and $R=20$)

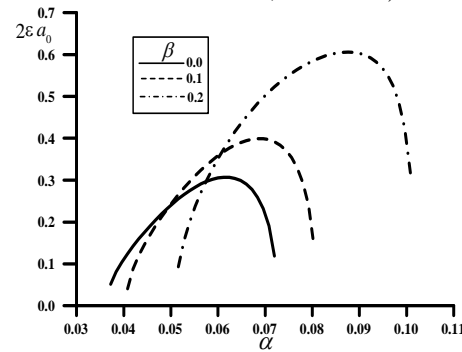


Fig. 6(b) Threshold amplitude in supercritical stable region for three different values of β . ($Re=8$, $m=0.2$, $k=0.1$, and $R=50$)

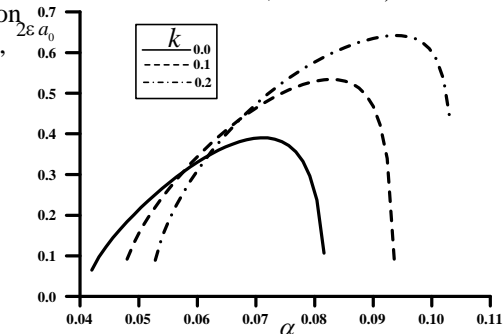


Fig. 6(c) Threshold amplitude in supercritical stable region for three different values of k . ($Re=8$, $m=0.1$, $\beta=0.1$, and $R=20$)

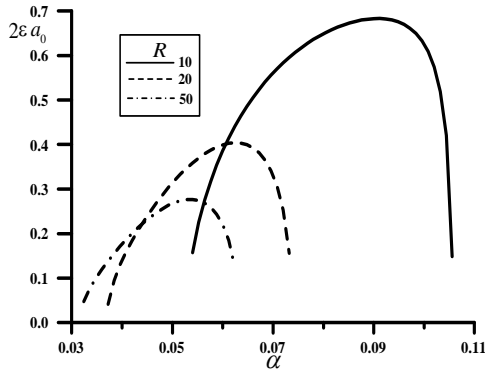


Fig. 6(d) Threshold amplitude in supercritical stable region for three different values of R . ($Re=5$, $m=0.2$, $\beta=0.1$, and $k=0.2$)

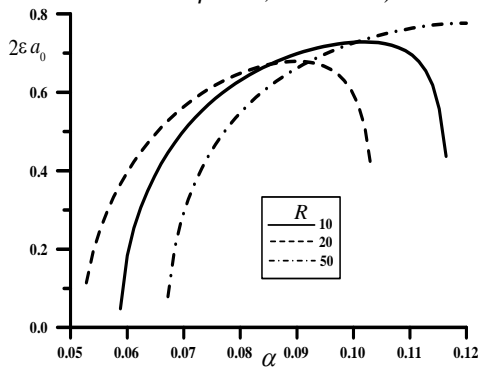


Fig. 6(e) Threshold amplitude in supercritical stable region for three different values of R . ($Re=5$, $m=0.2$, $\beta=0.5$, and $k=0.2$)

Figure 7 shows the relation between wave speed and nonlinear wave speed. The nonlinear wave speed can be obtained by Eq. (63). When the wave speed is slower, the thin film has better stability. Fig. 7(a) shows that both linear and nonlinear wave speed decreases with increasing Hartmann number. Fig. 7(b) and 7(c) show that higher Rossby number and viscoelastic parameter do not affect linear wave speed, but nonlinear wave speed has dramatic changes. In Fig. 7(d), linear wave speed does not change with radius under larger Rossby number (i.e., $\beta = 0.5$), but nonlinear wave speed does. When radius is respectively larger (i.e., $R = 50$), nonlinear wave speed has relatively higher maximum wave speed, and the thin film system is less stable.

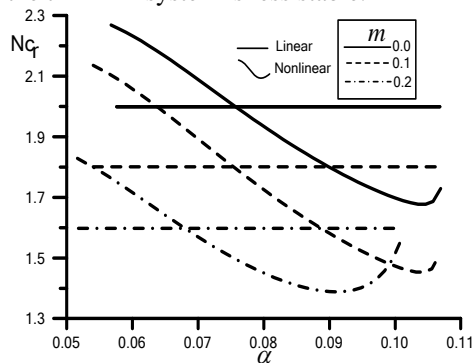


Fig. 7 (a) Nonlinear wave speed in supercritical

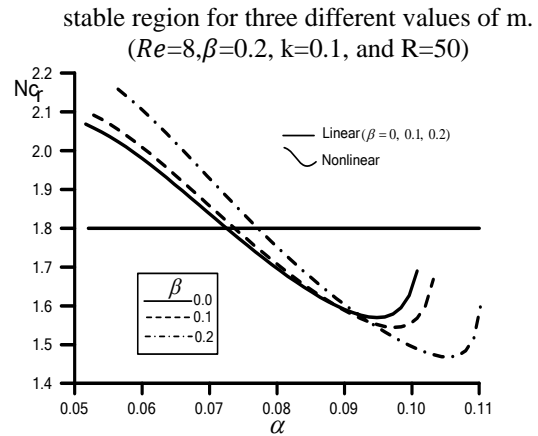


Fig. 7 (b) Nonlinear wave speed in supercritical stable region for three different values of β . ($Re=8$, $m=0.1$, $k=0.2$, and $R=20$)

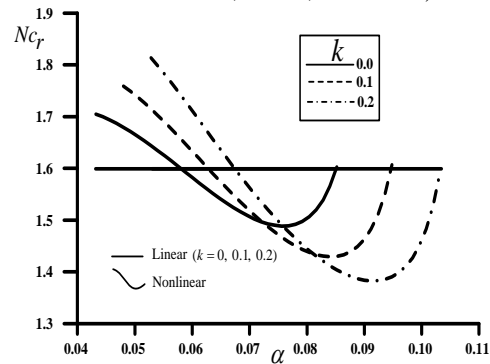


Fig. 7 (c) Nonlinear wave speed in supercritical stable region for three different values of k . ($Re=8$, $m=0.2$, $\beta=0.2$, and $R=20$)

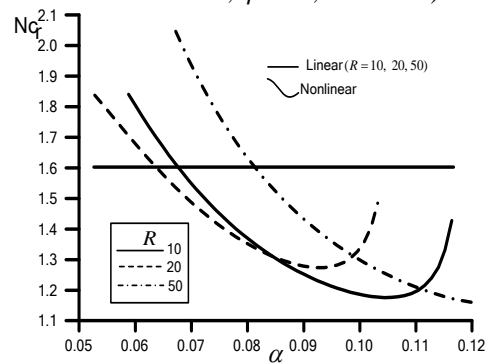


Fig. 7 (d) Nonlinear wave speed in supercritical stable region for three different values of R . ($Re=5$, $m=0.2$, $\beta=0.5$, and $k=0.2$)

The results above show that the trend in smaller radius is opposite to larger radius. When the radius is smaller, higher Hartmann number, lower Rossby number and lower viscoelastic parameter lead to a stable system. The system is not stable under larger radius. By Eq. (30), the streamwise surface tension term is independent of the cylinder radius R . The lateral surface tension term, on the contrary, varies inversely with R . As the result, for the model that has larger radius, the lateral surface tension becomes larger and

leads to lower stability of the thin film. The result from this paper matches the results from other studies written by other authors. The result of enhancing magnetic field, lower rotating velocity and lower viscoelasticity can increase stability under smaller radius matches the conclusion made by other authors (Cheng, 2009). If the effect of magnetic field is neglected, the results match the study done by other researchers that did not consider magnetic field (Chen et al., 2003).

CONCLUSIONS

This paper focused on thin electrically-conductive viscoelastic fluid film flowing on the surface of a rotating vertical cylinder in a magnetic field and discussed the stability of this system. The following results are obtained by using long-wave perturbation method on linear stability and nonlinear stability:

1. Enhancing magnetic field, lower rotating velocity and lower viscoelasticity can increase stability.
2. By enhancing magnetic field, lower rotating velocity and lower viscoelasticity, the subcritical instable region will expand, and supercritical instable region will shrink.
3. Subcritical and supercritical stable regions will be affected by magnetic field, rotating velocity and viscoelasticity. The area of the regions does not change very significantly, but the domain of Reynolds number and wave number will shift.
4. When the dimensionless radius is smaller, the stability of the thin film is dominated by Hartmann number, Rossby number and dimensionless viscoelastic parameter. When the dimensionless radius is larger, such as the dimensionless radius $R > 50$ or more, the lateral surface tension has greater influence on the stability of the thin film, which leads to much instable system.

REFERENCES

Ahmad, F., Gul, T., Khan, I., Saeed, A., Selim, M.M., Kumam, P., and Ali, I., "MHD thin film flow of the Oldroyd-B fluid together with bioconvection and activation energy"; *Case Studies in Thermal Engineering* 27, 101218, (2021).

Chen, C.K., Cheng, P.J., and Lai, H.Y., "Stability analysis of thin viscoelastic liquid film flowing down on a vertical wall"; *Journal of Physics D: Applied Physics* 33, 1674-1682, (2000).

Chen, C.I., Chen, C.K., and Yang, Y.T., "Weakly nonlinear stability analysis of thin viscoelastic film flowing down on the outer surface of a rotating vertical cylinder"; *International Journal of Engineering Science* 41, 1313-1336, (2003).

Chen, C.I., Chen, C.K., and Yang, Y.T., "Perturbation analysis to the nonlinear stability characterization of

thin condensate falling film on the outer surface of a rotating vertical cylinder"; *International Journal of Heat and Mass Transfer* 47, 1937-1951, (2004).

Chen, C.I., Chen, C.K., and Yang, Y.T., "Nonlinear stability analysis of thin Newtonian film flowing down on the inner surface of a rotating vertical cylinder"; *Acta Mechanica* 179, 227-248, (2005).

Chen, C.K., and Lin, M.C., "Weakly Nonlinear Stability Analysis of a Thin Liquid Film With Condensation Effects During Spin Coating"; *Journal of Fluids Engineering* 131, (2009).

Cheng, P.J., and Lin, D.T.W., "Surface waves on viscoelastic magnetic fluid film flow down a vertical column"; *International Journal of Engineering Science* 45, 905-922, (2007).

Cheng, P.J., "Hydromagnetic stability of a thin electrically conducting fluid film flowing down the outside surface of a long vertically aligned column"; *Proceedings of the Institution of Mechanical Engineers, Part C: Journal of Mechanical Engineering Science* 223, 415-426, (2009).

Dawar, A., Wakif, A., Thumma, T., and Shah, N.A., "Towards a new MHD non-homogeneous convective nanofluid flow model for simulating a rotating inclined thin layer of sodium alginate-based Iron oxide exposed to incident solar energy"; *International Communications in Heat and Mass Transfer* 130, 105800, (2022).

Edwards, D.A., Brenner, H., and Wasan, D.T., "Front Matter"; In *Interfacial Transport Processes and Rheology*, D.A. Edwards, H. Brenner, and D.T. Wasan, eds. (Butterworth-Heinemann), pp. iii (1991).

Ginzburg, V.L., and Landau, L.D., "Theory of superconductivity"; *J. Exp. Theor. Phys.*, (1950).

Khan, Z., Islam, S., Shah, R.A., Khan, M.A., Bonyah, E., Jan, B., and Khan, A., "Double-layer optical fiber coating analysis in MHD flow of an elastico-viscous fluid using wet-on-wet coating process"; *Results in Physics* 7, 107-118, (2017).

Lin, M.C., "Long-wave perturbation analysis to the stability of a thin viscoplastic material flowing on a rotating circular disk"; *International Journal of Engineering Science* 53, 112-123, (2012).

Tsai, J.S., Hung, C.I., and Chen, C.K., "Nonlinear hydromagnetic stability analysis of condensation film flow down a vertical plate"; *Acta Mechanica* 118, 197-212, (1996).

APPENDIX A

$$C_2 = S \text{Re}^{-2/3} (2\Gamma)^{1/3} \alpha^3 h R^2 (h - 2R) (h_z / q^2 + \alpha^2 h_{zz}) / \Omega - 4 \text{Re} \Gamma^2 h_z h^2 R^3 \Lambda \{160hR^4 - 480R^5 + 2h^3 R^2 (-93 + mR^2) + 14h^5 (1 + mR^2)(2 + mR^2) + 10h^2 R^3 (31 + mR^2) + h^4 R [91 + mR^2 (58 + 15mR^2)]\} k / (15q\Omega^2) + \text{Re} \beta^2 h_z h (h - 2R) R^4 / (2q\Omega) \quad (\text{A.1})$$

$$C_3 = 4h(h - 2R)R^4 \text{Re} \Gamma h_{zz} \Lambda / \Omega^3 + R \cdot S \text{Re}^{-2/3} (2\Gamma)^{1/3} \Phi (h_z / q^2 + \alpha^2 h_{zz}) / (3\Omega) + 4 \text{Re} \Gamma^2 h_z h R^2 \Lambda \{-600hR^5 + 240R^6 + 14h^5 (1 + mR^2)(2 + mR^2) + 40h^2 R^4 (4 + 3mR^2) + 10h^3 R^3 (55 + 7mR^2) - 2h^4 R^2 (153 + 29mR^2) + h^5 R [91 + mR^2 (58 + 15mR^2)]\} k / (45q\Omega^2) + \text{Re} \beta^2 h_z R^3 \Phi / (6q\Omega) \quad (\text{A.2})$$

受磁場影響的導電粘彈性 流體沿旋轉圓柱側流動的 薄膜穩定性分析

劉悟慢 陳朝光

國立成功大學機械工程學系

摘要

本文介紹了在磁場影響下的導電粘彈性流體薄膜沿旋轉垂直圓柱外側流下的流體穩定性研究。本文使用長波微擾法推導了液膜的廣義非線性運動方程。線性的薄膜穩定性條件會應用正模分析法來確定。最後使用多重尺度法來檢驗非線性穩定性。通過 Landau 方程式的不同係數判斷不同的流體薄膜狀態。由此可以得出，增加磁場強度，降低粘彈性效應，或者降低圓柱體旋轉速度可以增強流體薄膜的穩定性。與此同時，隨著圓柱半徑在大羅斯貝數(Rossby number)下的增加，如大於 50，流體薄膜會更容易失去穩定性，從而主導流體薄膜的狀態，導致其他參數對穩定性的影響降低。

$$C_1 = \text{Re}\{16R^2\Omega\Phi\Gamma h_{\omega}\Lambda + 24hR^3\Gamma\Lambda(2R-h)[\Omega h_{\omega} + 4h(h-2R)R^2\Gamma h_{\omega}] + [4R^2 + h(3h - 2R)(1+mR^2)](h_{\omega}/q^2 + \alpha^2 h_{\omega})S \text{Re}^{-5/3}(2\Gamma)^{1/3}\Omega^2\} - \text{Re}\Gamma^2 h_{\omega}\Lambda\{6240R^6 + 14h^6 (-1+mR^2)(1+mR^2)(2+mR^2) + 240hR^5(37+4mR^2) + 80h^2R^4(-2+41mR^2) + 2h^4R^2[-27+mR^2(-694+mR^2)] + 10h^3R^3[-271+mR^2(78+mR^2)] + h^5R(-1+mR^2)[91+mR^2(58+15mR^2)]\}k/(45q\Omega^4) + \text{Re}\beta^2 h_{\omega}R^2[h(2R-3h)(1+mR^2) - 4R^2]/(24q\Omega) \quad (\text{A.3})$$

$$C_2 = \text{Re}\{5h(h-2R)R^2q^2(1+3mR^2)\Lambda\Gamma h_{\omega} - 2(q+mhR^2)\Pi^2S \text{Re}^{-5/3}(2\Gamma)^{1/3}h_{\omega} - 40h(h-2R)R^2q^2\Lambda\Gamma^2h_{\omega} - 2(q+mhR^2)\Theta^2S \text{Re}^{-5/3}(2\Gamma)^{1/3}\alpha^2 h_{\omega}\}/(15q^2\Omega^3) + 4\text{Re}\Gamma^2 h_{\omega}\Lambda\{-2400R^7 + 14h^7(1+mR^2)(2+mR^2) - 120hR^6(197+10mR^2) - 60h^2R^5(419+118mR^2) + h^5(1548R^2 + 3328mR^4 - 298m^2R^6) + h^6R(2+mR^2)[91+mR^2(58+15mR^2)] - 20h^3R^4[104+mR^2(643+30mR^2)] - 10h^4R^4[-308+mR^2(378+89mR^2)]\}k/(225q\Omega^4) + \text{Re}\beta^2 h_{\omega}(R+h+mhR^2)R^2/(15q\Omega) \quad (\text{A.4})$$

and

$$\Theta = 2h^3 + mh^3R^2 + (2+mh^2)R^3, \quad \Lambda = h^2 + 2hR + (-2+mh^2)R^2 \quad (\text{A.5})$$

APPENDIX B

$$A(h) = -h^2\Gamma[28h^5 + 91h^4R + 42h^3R^2(-3+mh^2) + 2h^2R^3(65+29mh^2) + 2hR^4(80+mh^2 + 7m^2h^2) - 5R^5[48-mh^2(2+3mh^2)]]/(15q\Omega^2) \quad (\text{B.1})$$

$$B(h) = -3h^3 \text{Re}\alpha^2 \Gamma^2 \{[-80R^3 + 7h^3(1+mR^2) + 2h^2R(21+5mR^2)]S \text{Re}^{-5/3}(2\Gamma)^{1/3}\Omega^2 - 4h^3R^2q\Lambda[-3040hR^7 + 1920R^8 - 80h^2R^6(13+2mR^2) + 14h^5(1+mR^2)(2+mR^2)(1+3mR^2) - 32h^3R^5(-33+46mR^2) - 4h^4R^4[86+mR^2(-107+5mR^2)] + 2h^5R^3[313+mR^2(526+21mR^2)] - 2h^6R^2[19+mR^2(235+mR^2)(29+15mR^2)] + h^7R[203+mR^2(443+mR^2(161+17mR^2))]\}/(180q^3\Omega^5) + \text{Re}\alpha^2 h^4 \Lambda \{19200hR^7 - 24000R^8 + 56h^5(1+mR^2)(2+mR^2)^2 - 120hR^6 + 40h^3R^6(-709+75mR^2) - 80h^3R^5(1269+130mR^2) + 2h^7R(2+mR^2)[147+mR^2(116+65mR^2)] - 10h^4R^4[2253+mR^2(4522+145mR^2)] - 10h^5R^3[-1555+mR^2(1838+241mR^2)] + h^6R^2[6297+mR^2(14317-697mR^2 + 75m^2R^4)]\}k/(225q^2\Omega^4) + \text{Re}\alpha\beta^2 h^3 R^2[80R^3 - 7h^3(1+mR^2) - 2h^2R(21+5mR^2)]/(120q^2\Omega) \quad (\text{B.2})$$

$$C(h) = S \text{Re}^{-2/3}(2\Gamma)^{1/3} \alpha^3 h^3 [80R^3 - 7h^3(1+mR^2) - 2h^2R(21+5mR^2)]/(60\Theta) \quad (\text{B.3})$$

$$D(h) = h^2 \text{Re}\alpha^2 \Gamma^2 \{-3\Omega^4[80hR^5 - 240R^6 + 7h^6(1+mR^2)(2+mR^2) + 10h^5R^4(13+mR^2) + 8h^3R^3(10+9mR^2) + h^4R^2[35+3mR^2(22+5mR^2)] + h^5R[49+mR^2(52+19mR^2)]] S \text{Re}^{-5/3}(2\Gamma)^{1/3} - 2h^3R^2[62080hR^{13} - 46080R^{14} + 640h^2R^{12}(289+80mR^2) + 384h^3R^{11}(-289+133mR^2) + 70h^{14}(1+3mR^2)(2+3mR^2+m^2R^4) - 32h^4R^{10}[8536+mR^2(4903+215mR^2)] - 8h^5R^9[2551+mR^2(28752+6157mR^2)] + 12h^7R^7[3860+mR^2(13311+mR^2(3490-129mR^2))] + 120h^6R^4[795+mR^2(372+mR^2(-323+8mR^2))] + 2h^{13}R(1+mR^2)(2+mR^2)[532+mR^2(1411+5mR^2(168+53mR^2))] + 6h^9R^5[2343+mR^2[2802+mR^2[(2386+mR^2(1074-101mR^2))]]] + 4h^8R^6[4776+mR^2[5403+mR^2(7824-mR^2(1473+190mR^2))] + h^{11}R^3[1192+mR^2[9263+mR^2[19452+mR^2(9678+5mR^2(396-25mR^2))]]] + 2h^{10}R^4[5945+3mR^2[8182+mR^2[7278+mR^2(3002+mR^2(203-20mR^2))] + 3h^{12}R^2[664+mR^2[1457+mR^2[2176+7mR^2(346+mR^2(136+15mR^2))]]] \}/(90q^4\Omega^6) + h^3 \text{Re}\alpha^2 \Gamma^2 \{-576000hR^{12} + 38400R^{13} + 280h^{13}(1+mR^2)^2(2+mR^2)^3 + 1600h^3R^{10}(1739+302mR^2) - 960h^2R^{11}(-49+575mR^2) + 8h^{12}R(1+mR^2)(2+mR^2)^2[217+mR^2(172+107mR^2)] - 160h^4R^9[-10774+mR^2(8549+965mR^2)] - 40h^5R^8[143403+mR^2(79750+1831mR^2)] - 200h^6R^7[3453+mR^2(22186+mR^2(5901+160mR^2))] + 4h^7R^6[501978+mR^2(162293-mR^2(245268+19855mR^2))] + h^{11}R^2(2+mR^2)[18639+mR^2(62800+mR^2(44942+7mR^2(72+125mR^2)))] - 8h^8R^5[-44319+mR^2(-180770+mR^2(-29042+mR^2(14636+175mR^2)))] - h^9R^4[10077+mR^2(14944+mR^2(-10896+mR^2(9144+533mR^2)))] + 2h^{10}R^3[39105+mR^2(42026+mR^2(-6090+mR^2(8208+mR^2(-2519+150mR^2)))]\}k/(225q^3\Omega^5) + \text{Re}\alpha\beta^2 h^2 R^2[480R^6 - 21h^6(1+mR^2)(2+mR^2) - 20h^3R^4(21+mR^2) - 6h^4R^2(21+5mR^2) - 84h^3(R^3+mR^5) - 8h^5R[21+mR^2(19+6mR^2)]]/(120q^3\Omega^2) \quad (\text{B.4})$$

$$E(h) = -S \text{Re}^{-2/3}(2\Gamma)^{1/3} \alpha^3 h^2 [28h^5 + 91h^4R + 42h^3R^2(-3+mh^2) + 2h^2R^3(65 + 29mh^2) + 2hR^4(80+mh^2 + 7m^2h^2) - 5R^5[48-mh^2(2+3mh^2)]]/(30q\Omega^2) \quad (\text{B.5})$$